



Analytical Similarity Assessment of ABP 959 in Comparison with Eculizumab Reference Product

Katariina M. Hutterer¹ · Anna Ip² · Scott Kuhns² · Shawn Cao² · Mats Wikström² · Jennifer Liu¹

Accepted: 20 June 2021 / Published online: 22 July 2021
© The Author(s) 2021

Abstract

Background ABP 959 is one of the first proposed biosimilars to eculizumab reference product (RP), a recombinant IgG2/4_K monoclonal antibody (mAb) that binds human C5 complement protein and inhibits C5 cleavage to C5a and C5b, preventing the generation of the terminal complement complex C5b-9. Eculizumab RP is approved for the treatment of paroxysmal nocturnal hemoglobinuria, atypical hemolytic uremic syndrome, myasthenia gravis in patients who are anti-acetylcholine receptor antibody positive, and neuromyelitis optica spectrum disorder in patients who are anti-aquaporin-4 antibody positive.

Objectives The objective of this work was to comparatively assess analytical (structural and functional) similarity between ABP 959 and eculizumab RP using sensitive, state-of-the-art analytical methods capable of detecting minor differences in product quality attributes.

Methods Comprehensive analytical (structural and functional) characterization utilizing orthogonal techniques was performed using multiple lots of ABP 959 and eculizumab RP over several years applying > 40 state-of-the-art assays. Comparisons were performed to investigate the primary structure and post-translational modifications including glycans, higher-order structure, particles and aggregates, product-related structures and impurities, thermal stability and forced degradation, general properties, and biological properties mediated by target binding.

Results Results confirmed that ABP 959 had the same amino acid sequence, similar primary structure, higher-order structure, post-translational profiles, and the same protein content and concentration (e.g., ABP 959: 9.4–10.0; eculizumab EU: 9.4–10.0; eculizumab US: 9.3–10.3 mg/mL) as well as biological activity as eculizumab RP.

Conclusions Based on these results, it can be concluded that ABP 959 is analytically similar to eculizumab RP.

Key Points

ABP 959 is being developed as a biosimilar to eculizumab.

ABP 959 has been shown to be analytically similar to eculizumab reference product (RP) in structural and functional assessments.

The high degree of similarity in structure and function provides assurance that ABP 959 will likely be clinically similar to eculizumab RP.

✉ Jennifer Liu
jliu@amgen.com

¹ Biosimilar Process Development, Amgen Inc., One Amgen Center Drive, Thousand Oaks, CA 91320, USA

² Process Development, Amgen Inc., One Amgen Center Drive, Thousand Oaks, CA 91320, USA

1 Introduction

ABP 959 is a proposed biosimilar to eculizumab reference product (RP), a recombinant IgG2/4_k monoclonal antibody (mAb) that binds human C5 complement protein and inhibits C5 cleavage to C5a and C5b, preventing the generation of the terminal complement complex C5b-9 mediated proinflammatory signaling pathways and thrombus formation [1–3]. Eculizumab RP is approved for the treatment of patients with paroxysmal nocturnal hemoglobinuria, atypical hemolytic uremic syndrome, anti-acetylcholine receptor antibody positive myasthenia gravis, and anti-aquaporin-4 antibody positive neuromyelitis optica spectrum disorder (adult patients) [1, 3].

ABP 959 and eculizumab RP molecules contain constant regions from human IgG2 Fab and hinge and IgG4 Fc sequences and murine complementarity-determining regions (CDRs) grafted onto the human framework light chain and heavy chain variable regions. ABP 959 is being developed to have the same amino acid sequence, strength, and presentations as the approved eculizumab RP.

While eculizumab RP is manufactured using murine myeloma cells (NS0), ABP 959 is produced from Chinese hamster ovary (CHO) cells. Proteins from both cell lines contain post-translational modifications including glycans commonly seen in human proteins. The CHO cell line primarily expresses mAbs containing N-acetylneuraminic acid (NANA), common to human proteins, and does not produce mAbs containing the non-human glycan galactose- α 1,3-galactose (α -gal). The NS0 line produces mAbs with human as well as non-human glycans (e.g., α -gal, N-glycolylneuraminic acid) [4].

Development of a biosimilar begins with comprehensive comparative analytical characterization, including structural and functional assessments, of the proposed biosimilar with the RP. This is followed by non-clinical assessments, human pharmacokinetic and pharmacodynamic evaluations, and finally a comparative clinical safety and efficacy study in a representative indication [5–8].

Analytical assessment forms the foundation of biosimilar development and is designed to evaluate critical quality attributes that can affect safety, potency, pharmacokinetics, and overall quality [6, 7]. This assessment incorporates a range of complementary state-of-the-art analytical techniques to ensure similarity in structure and function of the proposed biosimilar with the RP.

The objective of this work was to assess the analytical (structural and functional) similarity between ABP 959 and eculizumab RP. For these studies, the RP was sourced from the United States (eculizumab US) and from Europe (eculizumab EU) as recommended in regulatory guidance for biosimilar development [6, 7].

2 Materials and Methods

2.1 Samples for Analysis

ABP 959 was manufactured by Amgen, Inc. Eculizumab RP was sourced from the United States and the European Union (Soliris[®], Alexion Pharmaceuticals, Inc.). Multiple lots of eculizumab RP from US and EU regions were procured over time and stored, handled according to the manufacturer's instructions, and tested as part of the similarity assessment plan.

2.2 Electrospray Ionization Time-of-Flight Mass Spectroscopy (ESI-TOF-MS)

Intact protein samples were separated from buffer components, introduced to the mass spectrometer by reversed-phase high-performance liquid chromatography (RP-HPLC; Agilent 1200) and detected using a pre-tuned and calibrated time of flight (TOF) mass spectrometer (Agilent G6224A). The resulting summed ion spectra were deconvoluted to produce molecular mass profiles. The theoretical intact molecular weight calculations assumed that most of the C-terminal lysine residues on the heavy chain were processed, the N-termini of the heavy chain were cyclized to pyroglutamic acid, all cysteines were bridged, and all disulfides were intact.

For reduced and deglycosylated heavy and light chain mass analyses, samples were deglycosylated with peptide-N-glycosidase F (PNGase F; QA-Bio), denatured with guanidine hydrochloride, and then reduced with dithiothreitol. The samples were separated from buffer components and introduced to the TOF mass spectrometer via RP-HPLC. Summed ion spectra were deconvoluted to produce molecular mass profiles, which were compared with theoretical mass values.

2.3 Reduced Tryptic Peptide Mapping

Samples were reduced with dithiothreitol, alkylated with sodium iodoacetic acid, and deglycosylated with PNGase F. Excess reagents were removed by gel-filtration desalting spin columns prior to digestion with trypsin at 37 °C for 35 min. Resulting peptides were separated on a C4 reversed phase column (Waters) using ultra-high performance liquid chromatography (UHPLC) with a gradient of acetonitrile in water. The eluted peptides were detected at 214 nm, and peaks were identified using a high-resolution mass spectrometer with an electrospray ionization source (Q Exactive Orbitrap Mass Spectrometer, ThermoFisher Scientific).

2.4 Non-reduced Tryptic Peptide Map Liquid Chromatography–Mass Spectrometry (LC–MS)

Samples were denatured with RapiGest (Waters Corporation), alkylated with *N*-ethylmaleimide (Calbiochem), and then digested with trypsin (Promega). A portion of the digest was then reduced using tris (2-carboxyethyl) phosphine hydrochloride. The fragments were separated by RP-HPLC on a C4 column (Waters) with a gradient of acetonitrile with 0.1% trifluoroacetic acid (TFA). The eluted peptides were detected at 215 nm and by total ion current. Peaks were identified using liquid chromatography-mass spectrometry (LC–MS) using a high-resolution mass spectrometer coupled with ultra-performance liquid chromatography (UPLC) via an electrospray ionization source (Q Exactive Orbitrap Mass Spectrometer, ThermoFisher Scientific).

2.5 Isoelectric Point

Isoelectric points were determined by capillary isoelectric focusing using a capillary electrophoresis separation instrument equipped with a neutral-coated capillary (Beckman Coulter). Samples were electrophoresed through a pH gradient produced by an ampholytic solution (GE Healthcare) until they reached the pH equal to their isoelectric point and then were mobilized and detected by ultraviolet (UV) absorbance (280 nm) as they passed through a detection window in the capillary. The isoelectric points of the sample peaks were determined using a linear regression between two isoelectric point marker peaks (ProteinSimple).

2.6 Extinction Coefficient

Extinction coefficients (EC) were determined experimentally using combinatorial analytical techniques involving amino acid analysis, UV spectrometry, and intact molecular weight analysis. The resulting experimentally determined EC values are within 5% between ABP 959 and eculizumab. Additionally, the experimentally determined EC values are within 10% of the theoretically determined EC value for eculizumab. Therefore, the theoretically determined EC value is used to determine protein concentration for both ABP 959 and eculizumab.

2.7 Non-reduced Reversed-Phase High-Performance Liquid Chromatography (nrRP-HPLC)

Samples were loaded onto a Zorbax 300 SB-C8 reversed-phase column (Agilent) with a mobile base gradient of increasing hydrophobicity to separate the disulfide structural isoforms. Disulfide variants were detected by absorbance at 214 nm, and relative percent area of each peak was

calculated by dividing the area of the individual peak by the total peak area.

2.8 Hydrophilic Liquid Interaction Chromatography (HILIC) Ion Trap Mass Spectroscopy

Samples were treated with PNGase (Prozyme), and free N-linked glycans were labeled with fluorescent tag 2-aminobenzoic acid (Sigma-Aldrich) at the reducing terminal *N*-acetylglucosamine. The fluorescently labeled oligosaccharides were separated by hydrophilic liquid interaction chromatography (HILIC) (Sigma-Aldrich) using acetonitrile mobile phase with an increasing gradient of ammonium formate in water and were detected using a fluorescence detector. Coupling the HILIC with an ion-trap mass spectrometer was performed for identification and verification of peaks against the expected glycan mass.

2.9 Far UV-Circular Dichroism (FUV-CD)

Far UV-circular dichroism (FUV-CD) was performed at ambient temperature using a Chirascan spectropolarimeter (Applied Photophysics, Ltd). Samples were diluted to approximately 1.3 mg/mL with product buffer prior to measurements using cuvettes with a path length of 0.01 cm in the spectral region (195–250 nm). The resulting spectra were corrected for protein concentration and contributions from buffer (recorded separately under identical conditions) and reported as circular dichroism (CD) ellipticity. Spectral similarity was quantitated using the Thermo OMNIC software QC compare function (ThermoFisher Scientific), where 100% similarity indicates identical spectra [9].

2.10 Near UV-Circular Dichroism (NUV-CD)

Near UV-circular dichroism (NUV-CD) measurements were made on a Chirascan spectropolarimeter (Applied Photophysics Ltd, Leatherhead, UK) at ambient temperature. Samples were diluted with product buffer to approximately 1.3 mg/mL. Measurements were performed using cuvettes with a path length of 0.5 cm. The spectra were recorded using step size 0.5 nm, bandwidth 1 nm, response time 2 s, and a 4-scan average, with wavelength range from 340 to 240 nm. The resulting spectra were corrected for protein concentration and contributions from buffer (recorded separately under identical conditions) and reported as CD ellipticity. Spectral similarity was quantitated using the Thermo OMNIC software QC compare function (Thermo Scientific), where 100% similarity indicates identical spectra [9].

2.11 Differential Scanning Calorimetry (DSC)

Differential scanning calorimetry (DSC) was performed using a VP-capillary differential scanning calorimeter (Microcal/Malvern Instruments). All samples were diluted to approximately 0.5 mg/mL with product buffer. Measurements were made in six replicates with scans completed from 10 to 100 °C using a scan rate of 60 °C/h. Data were analyzed using Origin software (Origin Lab Corporation) to determine the thermal transition temperature (T_m), and statistical analysis was done using JMP software (SAS).

2.12 High Accuracy Light Obscuration (HIAC LO) and Microflow Imaging (MFI)

High accuracy light obscuration (HIAC LO) was conducted using a HIAC 9703+ liquid particle counting system equipped with an HRLD-150 light sensor (Beckman Coulter Inc.) to assess concentration of subvisible particles in sizes of ≥ 2 , ≥ 5 , ≥ 10 , and ≥ 25 μm . Particle concentration results were reported as cumulative particle counts per mL.

Microflow imaging (MFI) was conducted using an MFI 5200 particle imaging system containing a flow cell and a digital camera (ProteinSimple) to assess particles sized ≥ 5 μm . To quantify product-related particles that were likely proteinaceous and thus possess a higher risk for immunogenicity, the ≥ 5 - μm particle data were further analyzed morphologically using an aspect ratio of 0.85. Cumulative particle counts per mL were reported.

2.13 Sedimentation Velocity Analytical Ultracentrifugation (SV-AUC)

The sedimentation velocity analytical ultracentrifugation (SV-AUC) analysis of solution-state self-association of high molecular weight (HMW) species was performed using a Beckman Coulter Proteome Lab XL-I instrument. Product solutions were diluted with formulation buffer to approximately 0.5 mg/mL and then centrifuged at 45,000 rpm. UV absorbance of the supernatant at 280 nm was recorded. The experiments were performed in double-sector centerpiece cell assemblies with quartz windows. Scans were collected at 20 °C without delay between them. The SV-AUC data were analyzed using SEDFIT [10], with the analysis, the frictional ratio, time invariant noise, and meniscus values allowed to float during the nonlinear least squares fit.

2.14 Hydrophobic Interaction Chromatography High-Performance Liquid Chromatography (HIC-HPLC)

Hydrophobic interaction chromatography high-performance liquid chromatography (HIC-HPLC) was performed using a

1200 HPLC system (Agilent) with a ProPac HIC-10, 5- μm particle size, 4.6 \times 100-mm column (ThermoFisher). Samples were injected neat into the HIC-HPLC system. The runs were performed at room temperature eluting with 1 M ammonium sulfate, 20 mM sodium acetate, at pH 5.0, with decreasing levels of ammonium sulfate used as the mobile phases. The flow rate was 0.4 mL/min with variants detected by absorbance at 220 nm. Relative percent area of each peak was calculated by dividing the area of the individual peak by the total peak area.

2.15 Size-Exclusion High-Performance Liquid Chromatography with Light Scattering Detection (SE-HPLC-LS)

Size-exclusion high-performance liquid chromatography with light scattering detection (SE-HPLC-LS) was performed using a 1100 HPLC system (Agilent) with TSK-GEL G3000SWxl, 5- μm particle size, 7.8 mm ID \times 300-mm length column (Tosoh Biosep, Merck KGaA). Samples were injected neat into the SE-HPLC-LS system. Runs were performed at room temperature with 100 mM sodium phosphate, 250 mM sodium chloride, and pH 6.8 buffer used as mobile phase; flow rate was 0.5 mL/min. Detectors included a HELEOS MALS detector (Wyatt Technology), an Optilab TrEX RI detector (Wyatt), and a UV detector (Agilent) set at 280 nm. The refractive index increment, $dn/dc = 0.185$ (mL/g), was used for calculation of molecular mass. Results were reported as the molar mass of monomer and HMW species using Wyatt ASTRA software.

2.16 Size Exclusion Ultra-High-Performance Liquid Chromatography (SE-UHPLC)

Single replicate samples were loaded onto a size exclusion column (BEH200, UPLC Column, 4.6 mm \times 150 mm, 1.7 μm ; Waters Corporation) and separated isocratically using the same mobile phase described in Sect. 2.15; eluent was monitored by UV absorbance.

2.17 Reduced Capillary Electrophoresis-Sodium Dodecyl Sulfate (rCE-SDS) and Non-Reduced Capillary Electrophoresis-Sodium Dodecyl Sulfate (nrCE-SDS)

Non-reduced samples were denatured with sodium dodecyl sulfate (SDS) at 60 °C for 5 min. Sample reduction was performed using β -mercaptoethanol ($\geq 98\%$) in the presence of SDS at 70 °C for 10 min. Following denaturation, samples were analyzed using an SDS-MW Analysis Kit (Beckman Coulter) and PA 800 Proteome Lab Protein Characterization System (Beckman Coulter). Samples were injected onto a 50- μm bare, fused silica capillary and separated based on

hydrodynamic size resulting from an applied electric field. Analytes were monitored by UV absorbance at 220 nm, and purity evaluated by determining the peak area of each species as the percentage of the total peak area.

2.18 Anion-Exclusion High-Performance Liquid Chromatography (AEX-HPLC)

Charge variants, including the profile (acidic, main, and basic) were assessed using anion-exclusion high-performance liquid chromatography (AEX-HPLC) (YMC Bio-Pro QZ-F), 100 × 4.6 mm ID, 5- μ m pore size). Negatively charged proteins bind to positively charged functional groups on the surface of the stationary phase by electrostatic forces under appropriate pH and are then eluted by increasing the ionic strength of the mobile phase. Purity was assessed by calculating the percent peak area of the integrated peaks.

2.19 Terminal Complement Complex (TCC) Inhibition Potency Assay

An enzyme-linked immunosorbent assay (ELISA) to quantify terminal complement complex (TCC) was used to measure the ability of ABP 959 and eculizumab RP to bind to and inhibit the activation of complement protein C5 in human serum. Samples were incubated with a fixed concentration of normal human serum (Quidel) in assay plate wells pre-coated with zymosan (Complement Technology). In the absence of a C5 inhibitor, zymosan coated onto the wells would activate normal human serum complement and bind the C5b-9 complex generated from terminal complement. After washing the plate wells, an alkaline phosphatase-labelled anti-C5b-9 antibody was incubated in the test wells, followed by another wash and then the addition of an alkaline phosphatase substrate solution (Sigma-Aldrich), and absorbance at 405 nm was measured. Test sample C5 inhibition potency was determined by comparing the test sample response to the response obtained with the reference standard (relative potency).

2.20 Hemolysis Inhibition

A hemolysis inhibition assay was developed to quantify the inhibition of erythrocyte lysis, an endpoint downstream of terminal complement activation. In this assay, varying concentrations of ABP 959 and/or eculizumab RP were incubated with a fixed concentration of normal human serum. This mixture was then incubated with chicken erythrocytes coated with rabbit anti-chicken erythrocyte antibodies (both: Rockland Immunochemicals). After incubation, the mixture was centrifuged for 2 min at 1000 \times g, and degree of hemolysis, which correlates with the amount of complement activation, was quantified by measuring absorbance (A405 nm) of

the hemoglobin released into the supernatant. Results were reported as percent relative hemolysis inhibition activity values.

2.21 C5 Binding

Relative binding activity, binding kinetics, and affinity for C5 were measured by surface plasmon resonance (SPR) using Biacore (now Cytiva) instrumentation in a C5 binding assay. The C5 protein, purified from human serum, was injected over test antibody surface at various concentrations. The binding sensorgrams were fitted globally with a 1:1 Langmuir model. The relative binding activity of test antibody was determined using its maximal response (R_{max}) relative to the R_{max} of the reference standard after normalization with their capture level. Conventional kinetic measurements for on-rates, off-rates, and affinity were also determined by this method.

2.22 FcRn Binding

The binding of ABP 959 and eculizumab RP to neonatal Fc receptor (FcRn) was determined using an amplified luminescent proximity homogenous assay (AlphaScreen[®], Perkin Elmer) comprising two steps. In the first step, the Fc region of ABP 959 competes with a fixed concentration of Fc-biotin in solution at pH 6.0 for binding to histidine-tagged FcRn (FcRn-His). The second step utilizes the AlphaScreen beads to detect bimolecular interactions. When FcRn-His captured on the acceptor beads binds to the Fc-biotin captured onto the donor beads, the two types of beads are brought into molecular proximity. Then a laser is applied, the donor beads complexed with acceptor beads convert ambient oxygen to single oxygen, and energy is transferred to the acceptor bead resulting in light production (luminescence). The assay measures the dose-dependent decrease in luminescence when an Fc-containing sample is added to a reaction containing FcRn-His and Fc-biotin. Test sample activity was determined by comparing the test sample response to the response obtained for the reference standard. Results were reported as percent relative binding.

3 Results

ABP 959 lots used for similarity assessment of each attribute were chosen based on the impact that the manufacturing process was expected to have on that attribute. For attributes primarily influenced by the drug substance manufacturing process (e.g., glycan profile, biological functions), a representative drug product lot for each independent drug substance was included; however, when a drug product lot was not available, the drug substance lot

was used. For attributes primarily influenced by the drug product manufacturing process (e.g., protein concentration and volume), data from all available drug product lots were included.

The similarity testing plan for ABP 959 is summarized in Table 1. Where possible, orthogonal methods were used to comprehensively analyze structural attributes and biological functions. Results of selected comparative assessments are shown.

3.1 Primary Structure

Primary structures of ABP 959 and eculizumab RP were investigated by several complementary characterization methods (Table 1). Results of the intact mass and reduced and deglycosylated heavy and light chain mass analyses are summarized in Table 2. The intact mass for ABP 959 and eculizumab RP were similar and matched the theoretical mass within 50 ppm (Table 2).

Table 1 Analytical similarity testing plan for ABP 959 and eculizumab reference product

Category	Attribute/assay and analytical techniques
Primary structure	Intact molecular mass and profile by ESI-TOF-MS
	Reduced and glycosylated molecular masses and profiles of heavy chain and light chain by ESI-TOF-MS
	Amino acid sequence and profile by reduced tryptic peptide map LC-MS
	Post-translational modifications by reduced peptide map
	Disulfide peptides and profile by non-reduced peptide map LC-MS
	Disulfide isoforms IgG2-A, IgG2-A/B, and IgG2-B by non-reduced RP-HPLC
	Glycan attributes, afucosylation, high mannose, α -galactosylation, β -galactosylation, sialylation, and profile by HILIC glycan map
	Isoelectric point and profile by cIEF
	Extinction coefficient by amino acid analysis and UV spectroscopy
Higher-order structure	Identity by ELISA
	Secondary structure and profile by FUV-CD
	Tertiary structure and profile by NUV-CD
Particles and aggregates	Thermal stability profile and T_m by DSC
	Subvisible particles by HIAC and MFI
	Submicron particles by DLS
	Solution-state self-association % monomer and profile by SV-AUC
Product-related substances and impurities	Multimers and aggregate size by SE-HPLC-LS
	Size variants by SE-HPLC, rCE-SDS, nrCE-SDS
	Charge variants by AEX-HPLC
Thermal stability and forced degradation	Hydrophobic variants by HIC-HPLC
	Thermal stability at 40 °C and 50 °C assessed by purity and potency assay
	Photo degradation assessed by purity and potency assay
General properties	Protein concentration by UV spectroscopy
	Volume by gravimetric measurement
Biological activities	Potency by TCC formation inhibition
	Hemolysis inhibition in chicken erythrocyte
	C5 binding affinity and on- and off-rates by SPR
	FcRn binding activity by AlphaScreen
	Fc γ R2a binding activity by SPR
	Fc γ R2b binding activity by SPR
Lack of Fc γ R1a, Fc γ R3a, Fc γ R3b, and C1q binding activities	

AEX-HPLC anion exclusion-high-performance liquid chromatography, *cIEF* capillary isoelectric focusing, *DLS* dynamic light scattering, *DSC* differential scanning calorimetry, *ELISA* enzyme-linked immunosorbant assay, *ESI-TOF-MS* electrospray ionization time-of-flight mass spectroscopy, *FUV-CD* far ultraviolet circular dichroism, *HIAC* high-accuracy light obscuration, *HIC-HPLC* hydrophobic interaction chromatography-high-performance liquid chromatography, *HILIC* hydrophilic interaction liquid chromatography, *LC-MS* liquid chromatography-mass spectrometry, *MFI* microflow imaging, *nrCE-SDS* nonreduced capillary electrophoresis-sodium dodecyl sulfate, *NUV-CD* near ultraviolet circular dichroism, *rCE-SDS* reduced capillary electrophoresis-sodium dodecyl sulfate, *RP-HPLC* reversed-phase high-performance liquid chromatography, *SE-HPLC-LS* size-exclusion high-performance liquid chromatography with light scattering, *SPR* surface plasmon resonance, *SV-AUC* sedimentation velocity-analytical ultracentrifugation, *TCC* terminal complement complex, T_m thermal transition temperature, *UV* ultraviolet

Table 2 Summary of analytical similarity assessment results for selected attributes for ABP 959 and eculizumab reference product

Attributes	ABP 959 Range (<i>n</i>)	Eculizumab EU Range (<i>n</i>)	Eculizumab US Range (<i>n</i>)
Intact molecular weight (difference, ppm)			
Glycosylation: A1G0F: A2G0F (147666)	1–9 (3)	1–11 (3)	13–16 (3)
Glycosylation: A2G1F: M5 (147803)	8–12 (3)	2–5 (3)	5–9 (3)
Glycosylation: A2G0F: A2G0F (147869)	38–42 (3)	32–35 (3)	35–38 (3)
Glycosylation: A2G0F: A2G1F (148031)	4–21 (3)	4–20 (3)	0–10 (3)
Glycosylation: A2G1F: A2G1F (148194)	3–20 (3)	1–13 (3)	3–13 (3)
Glycosylation: A2G1F: A2G2F (148356)	12–18 (3)	32–49 (3)	15–35 (3)
Reduced and deglycosylated light chain (23134 Da) (difference, ppm)	1–22 (3)	–22 (3)	1–22 (3)
Reduced and deglycosylated heavy chain (49374 Da) (difference, ppm)	11–21 (3)	1–31 (3)	31–41 (3)
Reduced and deglycosylated heavy + Lys (49502 Da) (difference, ppm)	13–23 (3)	3–23 (3)	3–13 (3)
Glycan profile (%)			
α-Galactosylation	0.0 (10)	0.7–1.5 (17)	0.5–2.1 (24)
β-Galactosylation	19.5–34.6 (10)	14.6–22.1 (17)	0.8–24.1 (24)
High mannose	3.2–5.5 (10)	3.5–6.1 (17)	3.0–6.0 (24)
Afucosylation	0.9–1.0 (10)	0.9–2.3 (17)	1.5–2.5 (24)
Sialylation	0.3–0.8 (10)	2.7–4.4 (17)	2.4–5.0 (24)
NUV-CD spectral similarity (%) ^a			
Eculizumab EU	98.80–99.15 (3)	99.69–100 (3)	99.23–99.47 (3)
Eculizumab US	97.72–98.02 (3)	99.23–99.72 (3)	99.11–100 (3)
FUV-CD spectral similarity (%) ^a			
Eculizumab EU	99.90–99.96 (3)	99.95–100 (3)	99.95–99.97 (3)
Eculizumab US	99.91–99.96 (3)	99.95–99.99 (3)	99.95–100 (3)
Differential scanning calorimeter (°C)			
T_{m1}	70.1–70.2 (3)	70.1–70.1 (3)	70.0–70.1 (3)
T_{m2}	79.4–79.4 (3)	79.3–79.4 (3)	79.3–79.4 (3)
Subvisible particle concentration (HIAC)			
≥ 2 μM particles/mL	39–454 (10)	83–860 (13)	28–1861 (17)
≥ 5 μM particles/mL	9–108 (10)	8–318 (13)	8–629 (17)
≥ 10 μM particles/mL	1–18 (10)	3–17 (13)	0–248 (17)
≥ 25 μM particles/mL	0–3 (10)	0 (13)	0–2 (17)
Subvisible particle concentration (MFI)			
≥ 5 μM particles/mL	6–114 (10)	26–678 (13)	24–1652 (17)
≥ 5 μM non-spherical particles/mL	6–78 (10)	18–510 (13)	2–1398 (17)
SE-HPLC-LS size variants (kDa)			
High molecular weight peak	296–391 (3)	280–292 (3)	283–321 (3)
Main peak	138–139 (3)	138–139 (3)	138–139 (3)
Protein concentration (mg/mL)	9.4–10.0 (10)	9.4–10.0 (19)	9.3–10.3 (24)

EU European Union, FUV-CD far ultraviolet circular dichroism, HIAC high-accuracy light obscuration, MFI micro-flow imaging, *n* number of lots, NUV-CD near ultraviolet circular dichroism, SE-HPLC-LS size-exclusion high-performance liquid chromatography, T_m thermal transition temperature, US United States

^aThe 100% similarity for the NUV-CD and FUV-CD similarity scores indicate that these particular data sets were used as the reference in the comparisons

The predominant species in the intact mass analysis profile (Fig. 1a) were consistent with the presence of core fucosylated complex N-linked glycans with 0, 1, or 2 terminal galactose residues per heavy chain. For example, the mass of the most abundant species, labeled as peak C, was consistent with a structure that has a core fucosylated complex

N-glycan on each heavy chain, with 0 terminal galactose on both heavy chains (A2G0F:A2G0F). The molecular masses of reduced and deglycosylated products provided further evidence that the heavy chain and light chain polypeptide compositions of ABP 959 and eculizumab RP were similar and also matched the theoretical mass within 50 ppm

Fig. 1 Primary structure comparisons of ABP 959 and eculizumab reference product (RP). **a** Intact molecular mass profile by electrospray ionization time-of-flight mass spectroscopy, **b** Glycan map by hydrophilic interaction liquid chromatography—high-performance liquid chromatography. *EU* emission units, *Eculizumab EU* eculizumab RP sourced from the European Union, *eculizumab US* eculizumab RP sourced from the United States

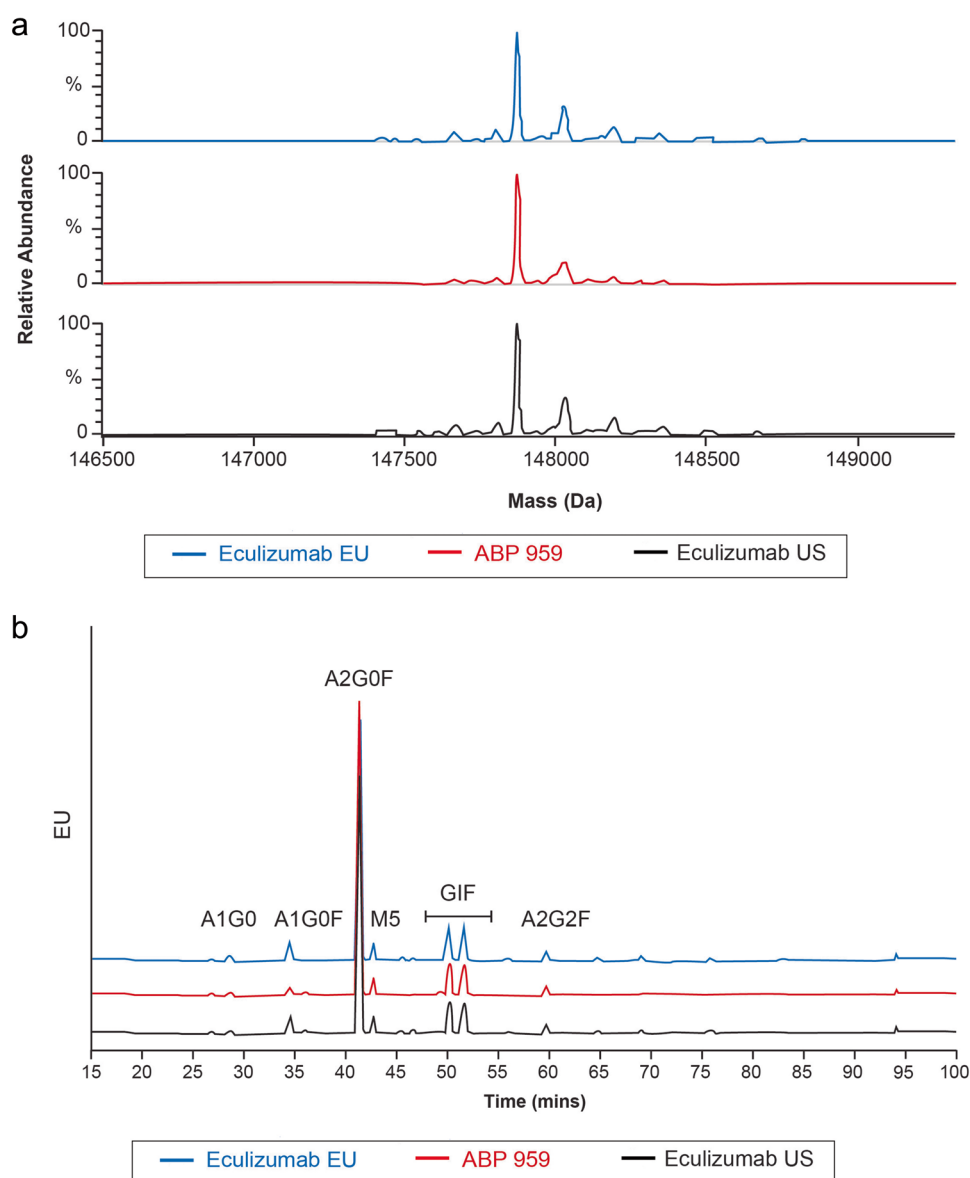


(Table 2). The complete amino acid sequence was confirmed by overlapping peptide maps with MS/MS data to ensure 100% coverage of the protein sequence.

The glycosylation profiles for ABP 959 and eculizumab RP from HILIC HPLC were similar (Fig. 1b). A total of 31 and 30 glycan structures have been identified for ABP 959 and eculizumab RP, respectively. Predominant glycan structures appeared to be core fucosylated, complex-type, bi-antennary structures with 0 or 1 galactose. The proportion of glycan groups classified as high mannose, afucosylation, α -galactosylation, β -galactosylation, and sialylation for each product is shown in Table 2. ABP 959 and eculizumab RP were found to have a similar level of high mannose and afucosylation, and a higher level of β -galactosylation. Because eculizumab RP does not exhibit effector function, no impact on biological activity is expected. As expected, the sialylated

glycans in ABP 959, produced by CHO cells, contained NANA while eculizumab RP, produced by NS0 cells, had sialylated glycans containing *N*-glycolylneuraminic acid (NGNA). Detection of low levels of α -gal in eculizumab RP and its absence in ABP 959 was also expected.

Other major post-translational modifications observed from the reduced peptide map were tryptophan and methionine oxidations located at M⁴, M⁴⁸, M⁸¹, W³³, W¹⁰⁷, M²⁵³, M³⁵⁹, and M⁴²⁹; all were < 2%. Isomerization was observed at D⁵⁶, D¹⁶⁷, D²⁸¹, and D⁴⁰²; all were < 0.5%.

The reduced peptide map also confirmed the single glycosylation site at heavy chain asparagine 298. The N-terminal glutamine (Q) residue on the heavy chain was predominantly in the pyroglutamic acid form for both ABP 959 and eculizumab RP. The C-terminal lysine-containing peptide was in low abundance, suggesting both C-termini of the heavy

chain predominantly end with the penultimate glycine, with the C-terminal lysine processed.

The disulfide structures of ABP 959 and eculizumab RP, determined from non-reduced tryptic peptide maps, were both confirmed to be consistent with the expected IgG2 disulfide structure for the Fab and hinge regions (Fig. 2); the location of disulfide peaks and corresponding cysteine residues and antibody chain locations are shown in Fig. 2a for the nonreduced (upper panel) and reduced peptide maps (lower panel). Both disulfide-linked peptides and reduced peptides were confirmed by mass spectrometry and structurally confirmed as shown in Fig. 2b. Peptide map overlays for the drug products (Fig. 2a) showed similar peak profiles with no new or missing peaks. Quantitative analysis of levels of the disulfide structures IgG2-A, IgG2-A/B, and IgG2-B isoforms were further conducted using nrRP-HPLC (Fig. 3a). Relative levels of disulfide isoforms in ABP 959 were approximately 61.1% for IgG2-B (the dominant isoform), 24.1% for IgG2-A/B, and 1.9% for IgG2-A based on nrRP-HPLC analysis, and the three disulfide structure isoforms were found in eculizumab RP (US and EU) at similar levels. Schematics for the three disulfide structure isoforms of ABP 959 and eculizumab RP detected by nrRP-HPLC and characterized by peptide map analysis are shown in Fig. 3b.

ABP 959 and eculizumab RP had similar isoelectric points and charge distribution profiles; no unexpected peaks were observed. The experimentally determined extinction coefficient values from amino acid analysis using UV spectroscopy for ABP 959 and eculizumab RP were similar. A dual anti-idiotypic ELISA identity test confirmed that ABP 959 and eculizumab RP share common CDR structural and conformational characteristics.

3.2 Higher-Order Structure

The secondary structure of ABP 959 and eculizumab RP was analyzed using FUV-CD spectroscopy (Fig. 4a), which showed similar profiles. The spectrum was characterized by a minimum at 217 nm and a maximum at 200 nm, features that are typical for a folded protein containing beta-sheet secondary structure. The FUV-CD spectral similarities of all individual ABP 959 lots compared with eculizumab RP were > 95% (Table 2). The FUV-CD results demonstrated that ABP 959 and eculizumab RP contain similar well defined secondary structures.

The tertiary structure of ABP 959 and eculizumab RP was analyzed using NUV-CD spectroscopy. Figure 4b shows the overlaid NUV-CD profiles for ABP 959 and eculizumab RP, which demonstrate similarity in the tertiary structures. The spectrum was characterized by features at 293 and 286 nm attributable to tryptophan, at 285–270 nm attributable to tyrosine and tryptophan, and at 250–265 nm attributable to phenylalanine, superimposed over the

disulfide signal from 250 to 280 nm. The NUV-CD spectral similarities of all individual ABP 959 lots compared with eculizumab RP were > 95% (Table 2). The NUV-CD results demonstrated that ABP 959 and eculizumab RP contain highly similar tertiary structures.

The thermal stability of ABP 959 and eculizumab RP was analyzed using DSC. The visual similarity of the scans showed that ABP 959 and eculizumab RP have similar thermal and conformational stability (Fig. 4c). This was also confirmed by similar thermal melting temperatures T_{m1} and T_{m2} (Table 2). These results demonstrated that ABP 959 and eculizumab RP have similar thermal stability.

3.3 Particles and Aggregates

ABP 959 and eculizumab RP had similarly low amounts of subvisible particles in sizes of ≥ 2 , ≥ 5 , ≥ 10 , and ≥ 25 μm as measured by HIAC LO, and similarly low amounts of non-spherical particles in the ≥ 5 - μm size range as assessed by MFI. The concentrations for particles in sizes of ≥ 2 , ≥ 5 , ≥ 10 , and ≥ 25 μm are provided in Table 2.

3.4 Product-Related Substances and Impurities

The SE-UHPLC profiles depicting the individual size variants were visually similar with no new or missing peaks (Fig. 5a). The HMW peak was characterized as a dimer. Levels of the HMW and low molecular weight (LMW) peaks were very low, with LMW levels close to the lower limit of quantification (0.1%) of the method.

The assessment of size variants of ABP 959 and eculizumab RP was further characterized by SE-HPLC-LS and SV-AUC. The HMW peaks observed for both ABP 959 and eculizumab RP were predominantly composed of dimers at low level.

The rCE-SDS profiles, depicting the non-glycosylated heavy chain clips (LMW and mid-molecular weight), light chain, heavy chain, and HMW for ABP 959 and the eculizumab RP were visually similar (Fig. 5b).

The nrCE-SDS profiles under non-reduced but denaturing conditions, showing main peak and pre-peak for ABP 959 and eculizumab RP, were visually similar with no new or missing peaks (Fig. 5c).

The AEX-HPLC profiles obtained to characterize the charge variants were similar, and no new or missing peaks were observed.

HIC-HPLC profiles characterizing hydrophobic variants are shown in Fig. 5d. The profiles were similar with no new or missing peaks.

Fig. 2 Disulfide profile for ABP 959 and eculizumab reference product (RP). **a** Non-reduced (upper panel) and reduced peptide maps (lower panel) liquid chromatography–mass spectroscopy, **b** identification of disulfide peaks, corresponding cysteine residues, and antibody domains. *AU* absorbance units, *Eculizumab EU* eculizumab RP sourced from the European Union, *eculizumab US* eculizumab RP sourced from the United States

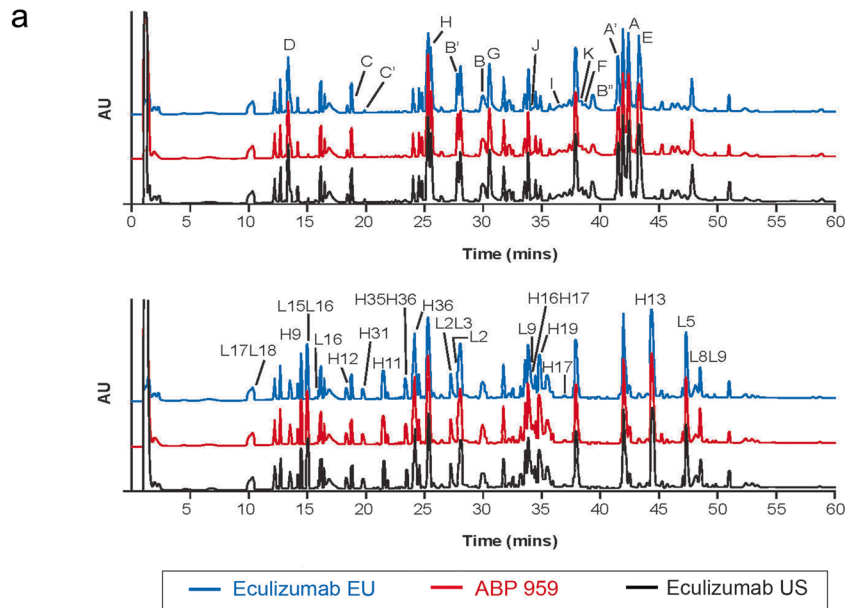


Fig. 3 IgG2 isoform profile for ABP 959 and eculizumab reference product (RP). **a** Non-reduced reversed-phase high-performance liquid chromatography (nrRP-HPLC), **b** schematic of the 3 disulfide structure isoforms of ABP 959 and eculizumab RP detected by nrRP-HPLC. Red and purple lines indicate disulfide bonds. *Eculizumab EU* eculizumab RP sourced from the European Union, *eculizumab US* eculizumab RP sourced from the United States, *mAU* milli-absorbance units

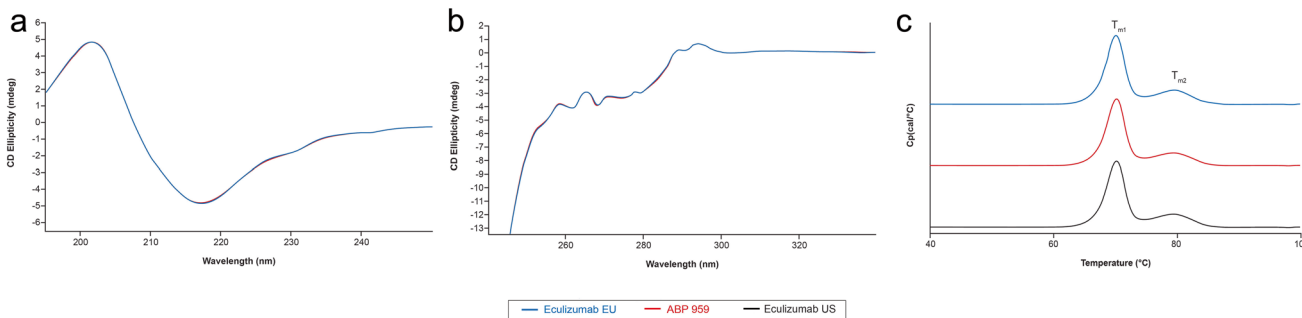
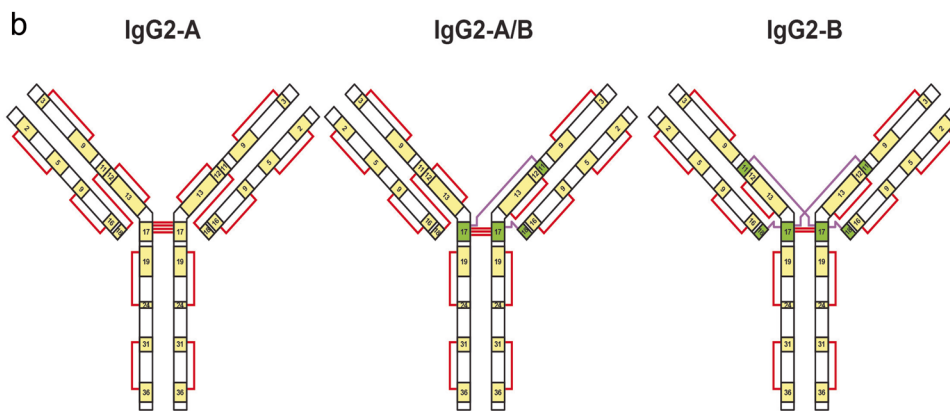
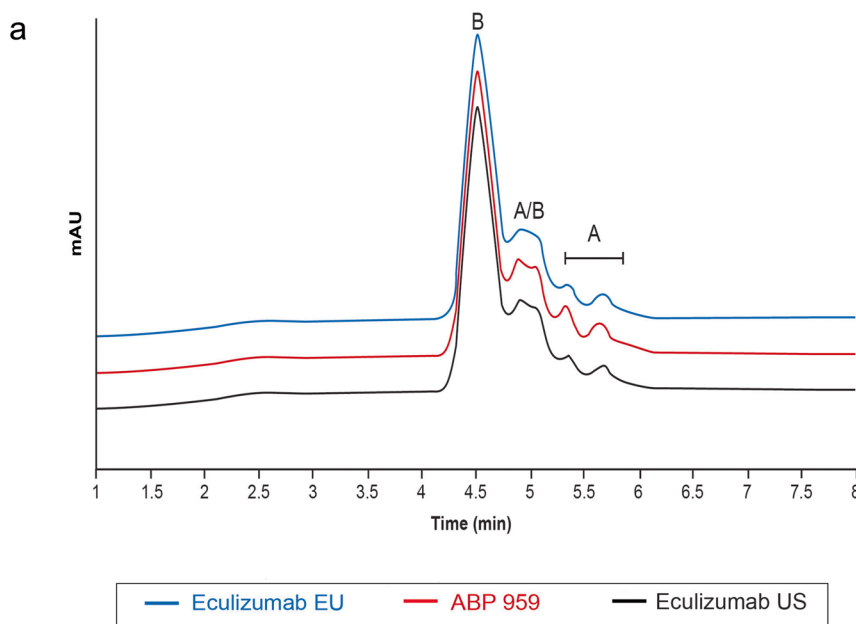


Fig. 4 Higher-order structure analysis of ABP 959 and eculizumab reference product (RP). **a** Far ultraviolet circular dichroism (UV-CD), **b** near UV-CD, **c** differential scanning calorimetry. *CD* circular

dichroism, *Cp* heat capacity, *Eculizumab EU* eculizumab RP sourced from the European Union, *eculizumab US* eculizumab RP sourced from the United States

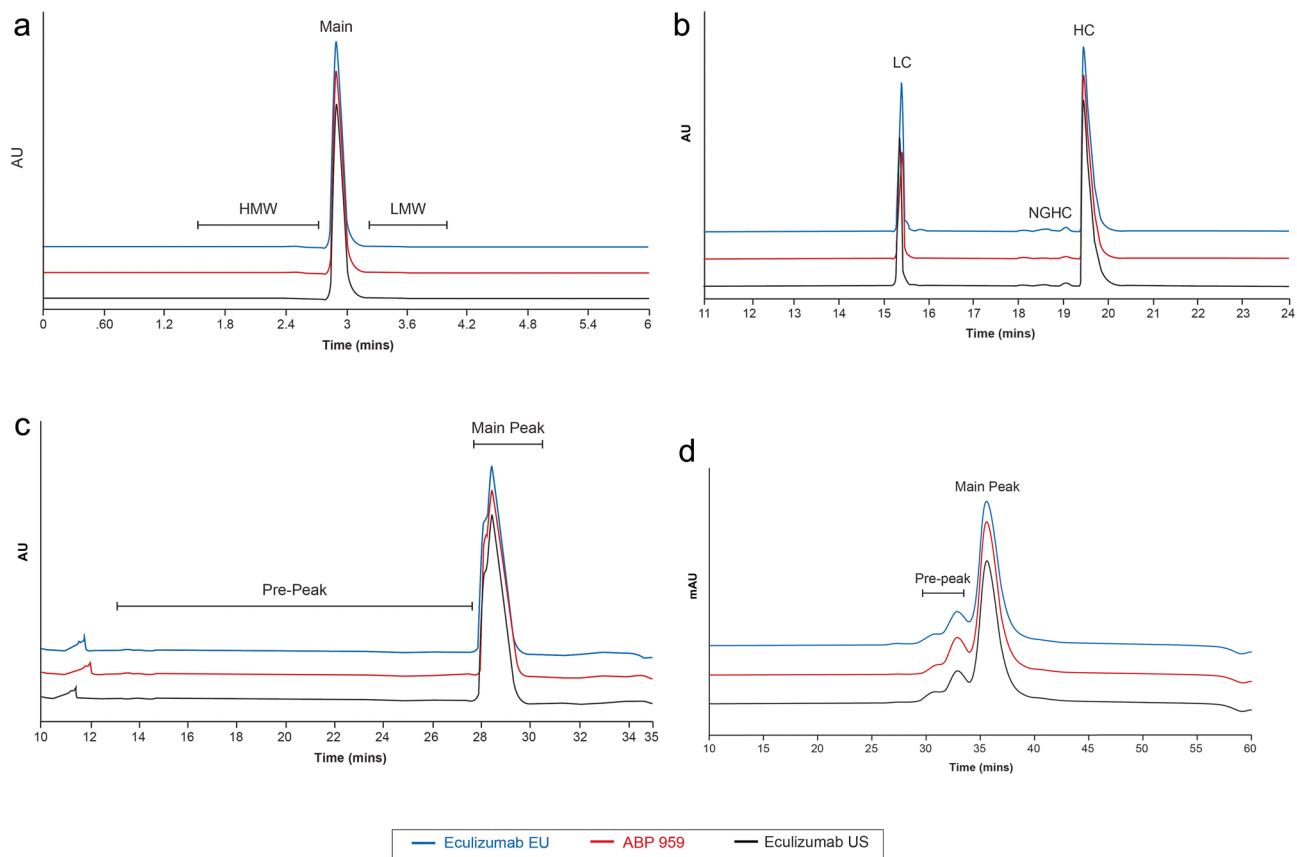


Fig. 5 Assessment of product-related substances and impurities for ABP 959 and eculizumab reference product (RP). **a** Size exclusion ultra-high-performance liquid chromatography, **b** reduced capillary exchange-dodecyl sulfate (CE-SDS), **c** non-reduced CE-SDS, **d** interaction chromatography—high-performance liquid chromatography.

AU absorbance units, *Eculizumab EU* eculizumab RP sourced from the European Union, *eculizumab US* eculizumab RP sourced from the United States, *HMW* high molecular weight, *LC* light chain, *LMW* low molecular weight, *mAU* milli-absorbance units, *NGHC* non-glycosylated heavy chain

3.5 General Properties

Protein concentrations for ABP 959 and eculizumab RP were similar as listed in Table 2. Results demonstrated that ABP 959 product strength was similar and consistent with eculizumab RP product label.

3.6 Biological/Functional Activity

Similarity of the biological activities of ABP 959 and eculizumab RP were evaluated with a combination of TCC formation inhibition potency assay by ELISA, hemolysis inhibition with chicken erythrocytes, C5 binding kinetics and affinity by SPR, and FcRn binding activity by a competitive binding assay. ABP 959 and eculizumab RP had similar effects on the biological activities as shown in Fig. 6a, b and Table 3.

Relative binding profiles for ABP 959 and eculizumab RP to C5 by binding assays and kinetic binding analysis were also similar (Table 3). FcRn binding properties were also

similar between ABP 959 and eculizumab RP; representative data are shown in Fig. 6c.

4 Discussion

An analytical strategy was developed and executed to comprehensively assess the structural and functional similarity of ABP 959 with its RP, which was sourced from the US and EU to satisfy the regulatory requirement of demonstrating similarity of the proposed biosimilar with the RP sourced from the local jurisdiction [6, 7]. Collectively, the RP lots included in the analytical similarity assessment represent the product profile over multiple years and captured the lot-to-lot variability as well as any potential drift due to any process changes. The ABP 959 lots were manufactured using the proposed commercial process and include clinical and development lots. The similarity assessment evaluated all critical and relevant attributes, including primary structure, higher-order structure, particles and aggregates,

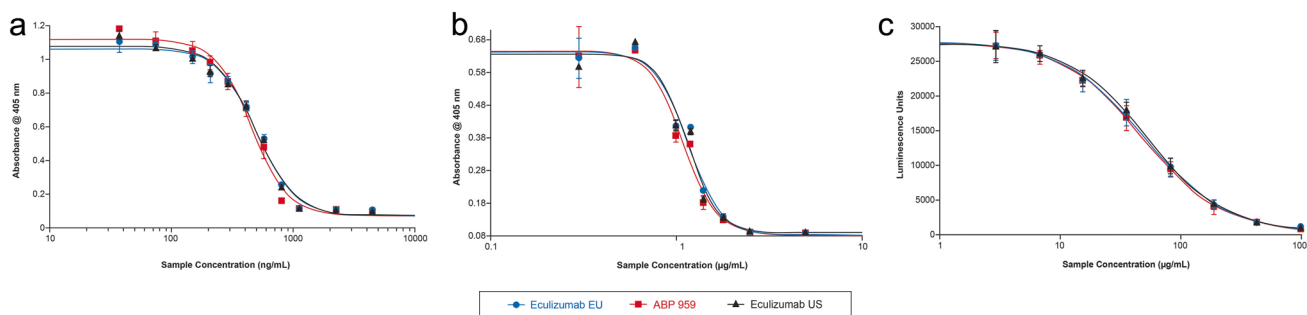


Fig. 6 Biological function of ABP 959 and eculizumab reference product (RP). **a** Inhibition of terminal complement complex (TCC) formation, **b** hemolysis inhibition, **c** FcRn binding. *Eculizumab EU*

eculizumab RP sourced from the European Union, *eculizumab US* eculizumab RP sourced from the United States

Table 3 Summary of biological and functional activities of ABP 959 and eculizumab reference product

Biological and functional activities	ABP 959 Range (n)	Eculizumab EU Range (n)	Eculizumab US Range (n)
Alternative complement pathway inhibition (relative potency, %)	93–115 (10)	95–124 (15)	92–134 (24)
Classical complement pathway inhibition (relative hemolysis, %)	99–109 (10)	99–111 (18)	96–111 (23)
C5 binding affinity (relative binding, %)	126–129 (3)	114–119 (3)	115–124 (3)
C5 binding kinetics (K_a , $M^{-1} s^{-1} \times 10^5$)	8.71–8.86 (3)	8.71–8.73 (3)	8.76–8.82 (3)
C5 binding kinetics (K_D , $s^{-1} \times 10^{-4}$)	1.00–1.04 (3)	1.10–1.12 (3)	1.01–1.09 (3)
FcRn binding activity (%)	98–106 (10)	95–102 (18)	94–106 (24)

K_a association constant, K_D dissociation constant

product-related substances and impurities, thermal stability and forced degradation, general properties, and biological activities, for both ABP 959 and eculizumab RP. For the assay and attributes considered critical to the clinical mechanism of action, pharmacokinetics, safety, and efficacy, orthogonal methods are employed to confirm similarity between ABP 959 and its RP. Based on the nature of the assay and attributes, appropriate pre-defined assessment criteria can be established. The assessment criteria established should be scientifically justified considering RP knowledge and RP data whenever available. Additionally, recent FDA guidance recommends risk assessment tools be developed to inform potential impact of an attribute on clinical performance, and to help inform the degree of uncertainty surrounding differences observed for specific quality attributes [11]. Efforts in these areas will further support analytical similarity between ABP 959 and eculizumab RP. To date, the results are consistent with ABP 959 being analytically and functionally similar to the eculizumab RP.

The intact molecular masses and results obtained from reduced and non-reduced peptide maps confirmed the expected identical amino acid sequence in ABP 959 and eculizumab RP. The disulfide linkage patterns for ABP 959

were similar to those for eculizumab RP and were based on the IgG2/G4_K hybrid structure containing IgG2 Fab and hinge and IgG4 Fc sequences as expected. Analyses also showed the expected disulfide bond-associated structural heterogeneity inherent to the IgG2 isotype class and the three isoforms characteristic of IgG2-A, IgG2-B, and IgG2-A/B, which differ by the pattern of the hinge region disulfide bonds [12].

The same post-translational modifications were detected in ABP 959 and eculizumab RP; the major modifications were tryptophan and methionine oxidations (2 tryptophan sites and 6 methionine sites), and isomerization at four aspartic acid sites, all at relatively low levels. Low-level deamidation and lysine glycation post-translational modifications were observed for both ABP 959 and eculizumab RP.

From the HILIC glycan map, five glycan groups (high mannose, afucosylation, α -galactosylation, β -galactosylation, and sialylation) were evaluated because of their potential to impact pharmacokinetics and biological functions. The glycan compositions of ABP 959 and eculizumab RP showed some differences primarily due to the CHO versus NS0 host cell lines used for ABP 959 and eculizumab RP, respectively. ABP 959 contained NANA

sialylation. In contrast, eculizumab RP had NGNA sialylation and low levels of α -galactose, which were absent in ABP 959. These differences were expected because ABP 959 and eculizumab RP are expressed from different cell lines: CHO for ABP 959 and NS0 for eculizumab RP. Both NS0 and CHO are mammalian cell lines frequently used in the commercial production of recombinant mAbs and other biologics with post-translational modifications, particularly glycosylation commonly seen in human proteins. The NS0 cell line also produces non-human glycans such as α -gal and N-glycolylneuraminic acid, whereas the CHO cell line primarily expresses NANA, commonly present in humans, and does not produce α -gal in the expressed mAbs [4]. During selection of the host-cell expression system for ABP 959, the known mechanism of action for eculizumab RP and the desired commercial manufacturing process efficiency of CHO cell lines were considered. The expected differences in glycosylation composition due to the change of host-cell expression systems have been fully characterized and assessed for potential impact on safety, efficacy, and quality. The absence of the non-human glycans in ABP 959 is not expected to have any clinically meaningful adverse effects. Also, the minor differences observed in the levels of afucosylation and galactosylation are not clinically meaningful, as ABP 959 and eculizumab RP do not have Fc effector functions. Importantly, the levels of high mannose, which affect pharmacokinetics, are similar in eculizumab RP and ABP 959.

ABP 959 and eculizumab RP also had similar secondary and tertiary structures. The spectral similarity of the FUV-CD and NUV-CD profiles were > 95%, which is the limit of the precision of the technology [13, 14]. Features of the FUV-CD spectral profiles for ABP 959 and eculizumab RP were similar and typical for a folded protein containing β -sheet secondary structure. The NUV-CD profiles for ABP 959 and the eculizumab RP were visually similar and consistent with the disulfide bonds and aromatic amino acids being in the expected environment due to the folding of the proteins. ABP 959 and eculizumab RP also had similar thermal and conformational stability and isoelectric points. While recent publications on 1D-NMR, 2D-NMR, and HDX-MS suggest these analytical technologies can provide further evidence in higher-order structure similarity for biosimilars, we believe our current analytical similarity study design, utilizing the combination of a large number of multidisciplinary analytical methods, provides a comprehensive structural and functional similarity assessment [14–17].

In the analysis of product-related substances and impurities, the level of HMW species size variants was slightly lower for ABP 959 than for eculizumab RP; this small difference is not expected to impact clinical efficacy. The ABP 959 AEX-HPLC chromatograms showed slightly higher levels of basic species and slightly lower levels of

acidic species compared with those for eculizumab RP. This is consistent with the quantitative results reported for capillary isoelectric focusing and is attributed to the larger proportion of C-terminal lysine species in the ABP 959 profile for basic species and the lower level of sialylation for the acidic species. These results were consistent with the peptide mapping and glycan mapping results and are not expected to influence overall biological activity. Finally, HIC-HPLC separated ABP 959 and eculizumab RP into the main peak and pre-peaks; the latter were enriched with C-terminal lysines, oxidized species, and high mannose species. Since the level of some product-related variants may change over the shelf-life, it is necessary to consider the material age at the time of testing when assessing similarity between biosimilar and the RP. In addition to comparing the product stability under the recommended storage condition, at 2–8 °C, stressed (40 °C) and forced degradation (50 °C) conditions were also used for the comparative analytical assessment to further probe similarity in structural and conformational integrity between the products.

Comparison of C5 binding profiles and effects on the TCC formation inhibition and hemolysis inhibition showed that ABP 959 and eculizumab RP have similar biological and functional properties relevant to the clinical mechanisms of action. ABP 959 and eculizumab RP also have similarly weak ability to activate Fc receptors and mediate complement activation. This is a desired characteristic of an antibody designed to inhibit complement activation and is consistent with its hybrid IgG2/4_k structure, with the IgG4 component comprising the Fc region [18].

5 Conclusion

The analytical similarity data presented here demonstrate that ABP 959 is structurally and functionally similar to eculizumab RP. Based on analytical characterization using state-of-the-art methods, ABP 959 has been shown to be structurally similar to eculizumab RP in primary and higher-order structure. Further, ABP 959 has also been shown to have similar biological and functional properties relevant to the clinical mechanisms of action to the RP based on C5 binding profiles and effects on the TCC formation inhibition and hemolysis inhibition. These findings provide justification for the further development of ABP 959 as an eculizumab biosimilar.

Acknowledgements The authors thank Mari Solveson, Nancy Jiao, Linda Collins, Rupa Padaki, Gwen Maher, Chris Rollins, and Sheeba Kazi (Amgen Inc., Thousand Oaks, CA) for experimental and scientific support. Medical writing support was provided by Annette F. Skorupa, Ph.D. (Innovation Communications Group, New York, NY) under the direction of Monica Ramchandani, Ph.D. (Amgen Inc., Thousand Oaks, CA).

Declarations

Funding This work was funded by Amgen Inc.

Conflict of interest All authors are employees and stockholders of Amgen Inc.

Ethics This article does not contain any studies with human participants or animals. All laboratory health and safety procedures have been complied with in the course of conducting this experimental work.

Author contributions KH: Led study design and assessment plan; authored the similarity plan; contributed to data interpretation, manuscript development, and review. AI: Contributed to study design and assessment plan; data acquisition, analysis, and interpretation; manuscript development. SK: Contributed to method development and testing; data analysis and interpretation; manuscript development. SC: Contributed to study design and assessment plan; protocol/methods development, data acquisition, analysis, and interpretation; manuscript development. MW: Contributed to study design and assessment plan; data acquisition, analysis, and interpretation; manuscript development. JL: Contributed to study design and assessment plan; development and authoring of manuscript.

Open Access This article is licensed under a Creative Commons Attribution-NonCommercial 4.0 International License, which permits any non-commercial use, sharing, adaptation, distribution and reproduction in any medium or format, as long as you give appropriate credit to the original author(s) and the source, provide a link to the Creative Commons licence, and indicate if changes were made. The images or other third party material in this article are included in the article's Creative Commons licence, unless indicated otherwise in a credit line to the material. If material is not included in the article's Creative Commons licence and your intended use is not permitted by statutory regulation or exceeds the permitted use, you will need to obtain permission directly from the copyright holder. To view a copy of this licence, visit <http://creativecommons.org/licenses/by-nc/4.0/>.

References

1. Soliris® (eculizumab RP) Injection, for intravenous use. Prescribing information. Alexion Pharmaceuticals, Inc. 2019. https://alexion.com/Documents/Soliris_USPI.pdf. Accessed 7 July 2020.
2. Corban MT, Duarte-Garcia A, McBane RD, Matteson EL, Lerman LO, Lerman A. Role of vascular endothelial cells and implications for risk stratification and targeted therapies. *J Am Coll Cardiol*. 2017;69:2317–30.
3. Soliris. Summary of product characteristics. European Medicines Agency. 2020 https://www.ema.europa.eu/en/documents/product-information/soliris-epar-product-information_en.pdf. Accessed 7 July 2020.
4. Dhara VG, Naik HM, Majewska NI, Betenbauch MJ. Recombinant antibody production in CHO and NS0 cells: differences and similarities. *BioDrugs*. 2018;32:571–84.
5. European Medicines Agency. Guideline on similar biological medicinal products (revision 1). 2014. https://www.ema.europa.eu/en/documents/scientific-guideline/guideline-similar-biological-medicinal-products-rev1_en.pdf. Accessed 12 Nov 2020.
6. European Medicines Agency. Guideline on similar biological medicinal products containing biotechnology-derived proteins as active substance: quality issues (revision 1). 2014. https://www.ema.europa.eu/en/documents/scientific-guideline/guideline-similar-biological-medicinal-products-containing-biotechnology-derived-proteins-active_en.pdf. Accessed 11 Feb 2021.
7. U.S. Department of Health and Human Services. Scientific considerations in demonstrating biosimilarity to a reference product. Guidance for industry. 2015. <http://www.fda.gov/downloads/Drugs/GuidanceComplianceRegulatoryInformation/Guidances/UCM291128.pdf>. Accessed 12 Nov 2020.
8. U.S. Department of Health and Human Services, Food and Drug Administration, Center for Drug Evaluation and Research, Center for Biologics Evaluation and Research. Quality considerations in demonstrating biosimilarity of a therapeutic protein product to a reference product. Guidance for industry. 2015. <http://www.fda.gov/downloads/drugs/guidancecomplianceregulatoryinformation/guidances/ucm291134.pdf>. Accessed 12 Nov 2020.
9. Li CH, Nguyen X, Narhi L, Chemmalil L, Towers E, Muzammil S, et al. Applications of circular dichroism (CD) for structural analysis of proteins: qualification of near- and far-UV CD for protein higher order structural analysis. *J Pharm Sci*. 2011;100:4642–54.
10. Schuck P. Size-distribution analysis of macromolecules by sedimentation velocity ultracentrifugation and Lamm equation modeling. *Biophys J*. 2000;78(3):1606–19.
11. U.S. Department of Health and Human Services, Food and Drug Administration, Center for Drug Evaluation and Research, Center for Biologics Evaluation and Research. Development of therapeutic protein biosimilars: comparative analytical assessment and other quality-related considerations. Guidance for Industry. 2019. <https://www.fda.gov/media/125484/download>. Accessed 6 May 2021.
12. Wypych J, Li M, Guo A, Zhang Z, Martinex T, Allen MJ, et al. Human IgG2 antibodies display disulfide-mediate structural isoforms. *J Biol Chem*. 2008;283:1619–25.
13. Li CH, Nguyen X, Narhi L, Chemmalil L, Towers E, Muzammil S, et al. Applications of circular dichroism (CD) for structural analysis of proteins. *J Pharm Sci*. 2011;100:4642–54.
14. Wen J, Batabyal D, Knutson N, Lord H, Wikström MA. Comparison between emerging and current biophysical methods for the assessment of higher-order structure of biopharmaceuticals. *J Pharm Sci*. 2020;109:247–53.
15. Elliott KW, Ghasriani H, Wikström M, Giddens JP, Aubin Y, Delaglio F, et al. Comparative analysis of one-dimensional protein fingerprint by line shape enhancement and two-dimensional ¹H, ¹³C methyl NMR methods for characterization of the higher order structure of IgG1 monoclonal antibodies. *Anal Chem*. 2020;92:6366–73.
16. Brinson RG, Marino JP, Delaglio F, Arbogast LW, Evans RM, Kearsley A, et al. Enabling adoption of 2D-NMR for the higher order structure assessment of monoclonal antibody therapeutics. *MAbs*. 2019;11:94–105.
17. Goswami D, Zhang J, Bondarenko PV, Zhang Z. MS-based conformation analysis of recombinant proteins in design, optimization and development of biopharmaceuticals. *Methods*. 2018;144:134–51.
18. Jefferis R. Antibody therapeutics: isotype and glycoform selection. *Exp Opin Biol Ther*. 2007;7:1401–13.